[1]R. Orbach and L. A. Vredevoe, Physics (Long Is. City) 1, 91 (1964).

[2]N. J. Zabusky, in *Nonlinear Partial Differential Equations*, edited by W. Ames (Academic, New York, 1967); N. J. Zabusky, J. Phys. Soc. Jap., Suppl. 26, 196 (1969).

[3]In cubic crystals, nearest-neighbor force constants of the type a_3 are zero on symmetry grounds.

[4]C. S. Gardner and G. K. Morikawa, New York University Institute of Mathematical Sciences Report No. 9082, 1960 (unpublished); C. H. Su and C. S. Gardner, J. Math. Phys. (N. Y.) 10, 536 (1969).

[5]R. Z. Sagdeev and A. A. Galeev, *Nonlinear Plasma Theory* (Benjamin, New York, 1969).

[6]R. M. Muira, J. Math. Phys. (N. Y.) 9, 1202 (1968); R. M. Muira, C. S. Gardner, and M. D. Kruskal, J. Math. Phys. (N. Y.) 9, 1204 (1968).

[7]D. J. Benney, J. Math. Phys. (Cambridge, Mass.) 46, 115 (1967); D. J. Benney and A. C. Newell, J. Math. Phys. (Cambridge, Mass.) 46, 133 (1967); D. J. Benney and G. J. Roskes, Stud. Appl. Math. 48, 377 (1969).

[8]V. I. Karpman, Pis'ma Zh. Eksp. Teor. Fiz. 6, 829 (1967) [JETP Lett. 6, 277 (1967)]; V. I. Karpman and E. M. Krushkal, Zh. Eksp. Teor. Fiz. 55, 530 (1968) [Sov. Phys. JETP 28, 277 (1969)].

[9]T. Taniuti and N. Yajima, J. Math. Phys. (N. Y.) 10, 1369 (1969); N. Asano, T. Taniuti, and N. Yajima, J. Math. Phys. (N. Y.) 10, 2020 (1969).

[10]L. A. Ostrovskii, Zh. Eksp. Theor. Fiz. 51, 1189 (1966) [Sov. Phys. JETP 24, 797 (1967)].

[11]S. A. Akhmanov, A. P. Sukhorukov, and R. V. Khokhlov, Usp. Fiz. Nauk 93, 19 (1967) [Sov. Phys. Usp. 10, 609 (1968)].

[12]P. L. Kelley, Phys. Rev. Lett. 15, 1005 (1965).

[13]N. J. Zabusky and M. D. Kruskal, Phys. Rev. Lett. 15, 240 (1965).

[14]D. J. Korteweg and G. de Vries, Phil. Mag. 39, 422 (1895).

[15]See for example, C. C. Ackerman and R. A. Guyer, Ann. Phys. (New York) 50, 128 (1968).

[16]T. F. McNelly *et al.*, Phys. Rev. Lett. 24, 100 (1970).

[17]V. Narayanamurti and C. M. Varma, preceding Letter [Phys. Rev. Lett. 25, 1105 (1970)].

ANISOTROPY OF THE ELECTRON-IMPURITY SCATTERING IN SOME DILUTE GOLD ALLOYS

D. H. Lowndes,* K. Miller, and M. Springford
School of Mathematical and Physical Sciences, University of Sussex, Brighton, England
(Received 2 June 1970)

A general method is described for obtaining a map of the variation of the electronic lifetime over the entire Fermi surface using the Dingle temperatures measured in the de Haas–van Alphen effect. The method is illustrated by presenting maps of the variation of the electron-impurity scattering lifetime for Au:Ag and Au:Fe dilute alloys.

We wish to present some preliminary results in which, for the first time, a map showing the detailed variation of the electronic lifetime over an entire Fermi surface has been obtained. We describe a conceptually simple and general analytical method for decomposing the orbitally averaged lifetimes measured in de Haas–van Alphen (dHvA) experiments to yield local values of the lifetime. The method requires a detailed knowledge of the topography of the Fermi surface and of the distribution of electronic velocities over it. Such information has recently become available for the noble metals[1] and we illustrate the method using two dilute alloys of gold, Au:Fe and Au:Ag, in which the scattering of electrons is dominated by the solute.

The determination of local values of the electronic lifetime over the Fermi surface in a metal is a problem of considerable current interest as evidenced by the many aspects of this problem reviewed in the published proceedings of a recent international conference.[2] For such determination, one requires ideally a physical effect which arises from a local and well-defined group of carriers. The application of one such effect, magnetic-field–induced quantum states, to study most elegantly the anisotropy of electron-phonon scattering in copper was reported recently in this journal.[3] The tilted-field Gantmakher effect has similarly been used in potassium.[4] While in principle such effects may be employed to study the scattering of electrons by imperfections other than phonons, their application is confined to materials of high purity relative to those which may conveniently be studied by means of the dHvA effect. The work reported here, while at an early stage, is intended to illustrate that the dHvA method may be used to explore in some detail the anisotropy of electron-impurity scattering for dilute alloys of relatively high solute concentrations. Demands upon material characterization are thus less stringent for the dHvA method which has the further advantage that problems inherent in the preparation of

suitably shaped samples for the surface state and Gantmakher techniques are also avoided.

One measures from the magnetic field dependence of the dHvA effect the scattering temperature or Dingle temperature, x, which is directly related to the scattering of electrons in states which lie along a narrow well-defined extremal orbit on the Fermi surface. Brailsford[5] relates x to the electronic lifetime τ at the Fermi surface, by the relation $x = \hbar/2\pi k_B\tau$. In general however, τ will vary over the Fermi surface, and the effective level width, $2\pi k_B x$, for a particular extremal orbit is then related to an average of the reciprocal lifetime around the relevant orbit,[6]

$$\langle \tau^{-1} \rangle = 2\pi k_B x/\hbar. \quad (1)$$

While a single measurement of x obscures the variation of lifetime around the orbit, the local lifetimes may be deduced from a series of such measurements for different but intersecting extremal orbits as follows.

Previous authors have not specified how the average in (1) is determined. However, in the most general case, the average scattering rate ($\propto$ transition probability) is obtained by summing the local scattering rates ($\propto$ local transition probabilities). Thus to calculate the orbital average in (1) we make the assumption that each local value of the electronic lifetime, $\tau(t)$, contributes in proportion to the amount of time dt spent by the wave vector $\vec{k}$ in each region along the Fermi surface orbit. So we write

$$\langle \tau^{-1} \rangle = T^{-1} \oint dt/\tau(t), \quad (2)$$

which may be expressed as a line integral,

$$\left\langle \frac{1}{\tau} \right\rangle = \frac{1}{T}\oint \frac{ds}{\dot{s}\tau(s)} = \frac{\hbar}{2\pi m^*}\oint \frac{ds}{\tau(s)v(s)\sin[\vec{v}(s), \vec{H}]} \quad (3)$$

using the Lorentz force equation where $\dot{s}$ is the tangential velocity along the orbit, $v(s)$ is the local Fermi velocity, and m^* is the cyclotron effective mass for the extremal orbit. η is an angle in a plane normal to H which specifies the orientation of the projection $k_\perp$ of the $\vec{k}$ vector on to this plane, for a state on the extremal orbit. Using reduced (free electron) units,[1] (3) becomes

$$\langle \tau^{-1} \rangle = (2\pi m^*)^{-1} \oint [d\eta/\tau(\eta)]\, W_A(\eta). \quad (4)$$

Here $W_A(\eta)$ is an anisotropic weight function

$$W_A(\eta) = \frac{k_\perp(\eta)[1 + (k_\perp^{-1} dk_\perp/d\eta)^2]^{1/2}}{v(\eta)\sin[\vec{v}(\eta), \vec{H}]} = \frac{k_\perp^2}{\vec{v}(\eta)\cdot\vec{k}_\perp}, \quad (5)$$

where $\oint W_A(\eta)d\eta = 2\pi m^*$, which may be evaluated at arbitrary orientations for the noble metals using the data of Halse[1] and consequently can be checked against experimental measurements of m^*. The determination of $\tau(\eta)$ thus reduces to the computational problem of self-consistently inverting integrals like (4) to fit Dingle-temperature measurements corresponding to a variety of different extremal orbits. Several inversion schemes may be suggested. Quite generally, one could express the local electronic lifetime parametrically in terms of an expansion in spherical harmonics of the appropriate symmetry, and then adjust the coefficients in the expansion to best fit the experimental data. A computer program can then be used to perform iteratively the least squares fitting of calculated to experimental orbital averages. An alternative approach, and one which we have adopted in this preliminary work in order to illustrate the method, is to construct a generalized model for the variation of the lifetime and again to best fit the parameters which describe the model by means of an iterative least-squares fitting procedure. Clearly, the results obtained by means of this second method can only be regarded as approximate. However, in addition to illustrating the principles of the method, such an analysis may be a useful preliminary to the more general approach, in revealing the gross features of the scattering anisotropy characteristic of a particular impurity.

The dilute gold alloys that we have investigated are 0.237 and 0.51 at.% Au:Ag and 190 ppm Au:Fe, as determined by both spectrographic analysis and residual resistivity ratio. Dingle temperatures have been measured for the five extremal orbits which are observed with the magnetic field along the [100], [110], and [111] axes in gold. For both computational and experimental reasons it was convenient in the initial experiments to confine measurements to these symmetry directions although in general this would not necessarily be the optimum procedure. Dingle temperatures per atomic percent of solute determined from these measurements, and from similar measurements for the pure solvent material, are summarized in Table I. A computer program was written to evaluate the W_A using the data of Halse[1] and to perform iteratively the least-squares fitting of calculated to experimental Dingle temperatures. A model expression was used for the lifetime anisotropy having the

Table I. Dingle temperature per atomic percent of solute in gold for five extremal orbits observed with the magnetic field along principal symmetry directions. Values determined from the dHvA effect, using the low-frequency field-modulation technique, are compared with those computed from the maps of $\tau(\vec{k})$ in Figs. 1 and 2.

	Au:Ag		Au:Fe	
	Experimental	Calculated	Experimental	Calculated
⟨100⟩ belly	6.81 ± 0.39	6.71	147 ± 10	147
⟨100⟩ rosette	5.48 ± 0.08	5.59	133 ± 13	113
⟨110⟩ dogsbone	5.85 ± 0.10	5.98	89 ± 5	89.3
⟨111⟩ belly	6.06 ± 0.12	5.90	123 ± 5	123
⟨111⟩ neck	2.12 ± 0.12	2.12	74 ± 4	74.3

general form

$$\tau_i^{-1} = \tau_0^{-1} + \sum_j \Delta\tau_j^{-1} \exp -(\theta_{ij}/\omega_j)^2, \qquad (6)$$

where τ_i is the local electronic lifetime at a general point i on the Fermi surface, τ_0 is a constant, and the summation is taken over the symmetry directions j = [001], [101], and [111], about which a Gaussian variation of lifetime is assumed of height τ_j and angular half-width ω_j. The polar coordinate θ_{ij} expresses the angular position of i with respect to the symmetry direction j, and the width ω_j need not be single valued but may be permitted to assume the symmetry appropriate to j. Consistent always with the number of fitted parameters being less than or equal to the number of measured Dingle temperatures, a variety of models based on (6) were used. It was evident that only for models which permitted the expression of certain principal features (e.g., a marked increase in the lifetime in the neck regions for Au:Ag or a marked decrease in the [101] regions for Au:Fe) could even a crude fit to the experimental data be accomplished. We show in Figs. 1 and 2 the results of the best fits to the experimental data in the form of topographic maps showing contours of constant lifetime. In Table I the measured scattering temperatures are compared with the scattering temperatures calculated from the maps and are seen to be in very good agreement. The main result to

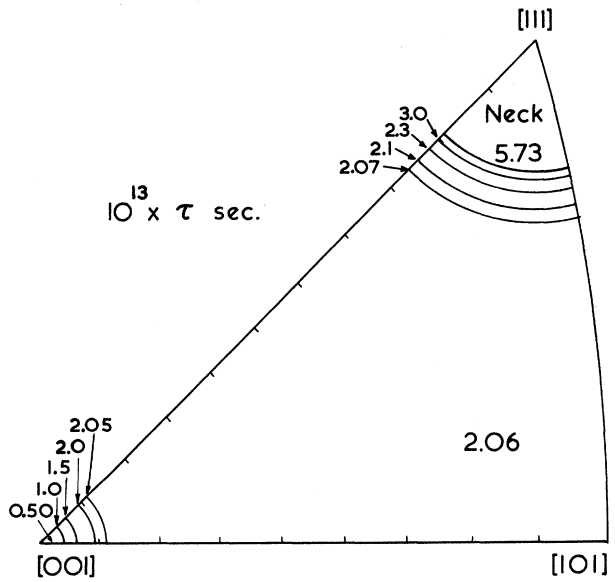

FIG. 1. Variation of the electronic lifetime over the Fermi surface in gold, per atomic percent of silver impurity. The figure depicts the basic, 1/48th, unit of the stereographic projection. The best-fit parameters in Eq. (6) are $\tau_0 = 2.06 \times 10^{-13}$, $\Delta\tau_{001} = 0.67 \times 10^{-13}$, $\Delta\tau_{101} = 0$, $\Delta\tau_{111} = -2.23 \times 10^{-15}$, $\omega_{111} = 4.1°$, and $\omega_{001} = 2.2°$.

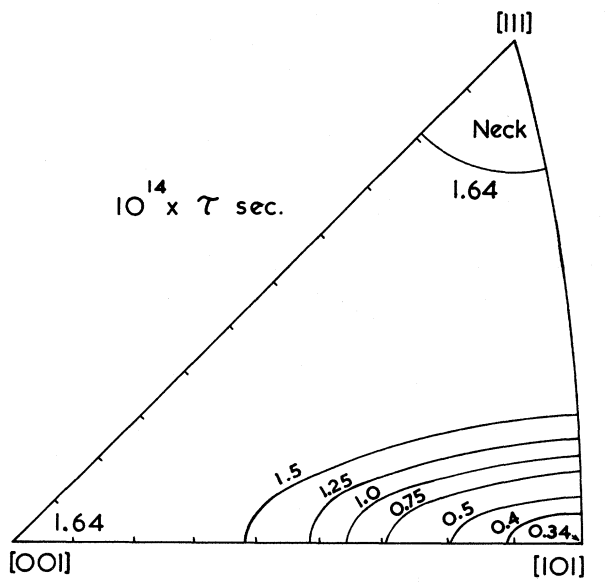

FIG. 2. Variation of the electronic lifetime over the Fermi surface in gold, per atomic percent of iron impurity. The figure depicts the basic, 1/48th, unit of the stereographic projection. The best-fit parameters in Eq. (6) are $\tau_0 = 1.64 \times 10^{-14}$, $\Delta\tau_{111} = 0$, $\Delta\tau_{101} = 4.25 \times 10^{-15}$, $\Delta\tau_{001} = 0$, $\omega_{101\text{-}001} = 13.25°$, and $\omega_{101\text{-}111} = 4.73°$.

be seen in these maps is that there exists a local, highly anisotropic electronic lifetime, and that this anisotropy is strikingly different in Au:Fe from that in Au:Ag.

Following Ziman,[7] the anisotropy of the relaxation time for Au:Ag may be qualitatively understood as being linked with underlying changes in the symmetry type, or hybridization of the electronic wave functions at different points on the Fermi surface. In particular, because wave functions for the electrons in the neck regions of the Fermi surface have nearly pure p character, these electrons are not strongly scattered by an uncharged impurity, such as Ag in Au, which is expected to produce only a very localized disturbance of the lattice potential and hence primarily s-wave scattering. Thus, for such an impurity, the lifetime of states in the belly (predominatly s-like) region of the Fermi surface is expected to be considerably shorter than in the neck (p-like) region as found in our Fig. 1 and in earlier comparisons of orbitally averaged neck and belly lifetimes.[8-10]

One can see that Ziman's argument is sufficiently general that is possible to extend it to consider other scattering centers; for example, a transition-metal impurity such as Fe in Au:Fe. Qualitatively, we expect particularly strong scattering in regions of the Fermi surface where the conduction-electron wave functions have been strongly admixed with functions having the same symmetry type as the impurity-induced disturbance to the lattice potential. In the nobel metals the anisotropy of the electronic lifetime can then also be linked with the anisotropy of the Fermi surface itself, that is, with its departures from sphericity, since these departures are also associated with changing wave-function symmetry throughout the Brillouin zone. The strongly increased scattering which we find near ⟨101⟩ in Au:Fe can be interpreted in terms of the corresponding distortion of the noble-metal Fermi surfaces near ⟨101⟩. This distortion is largest in Au and takes the form of a "pushing in" of the Fermi surface to form a large concave region extending from [101] toward [001]. This feature is clear in several Fermi surface calculations,[1,11-13] and is due to the strong admixture of a d-wave component into the electronic wave functions near the ⟨101⟩ directions.[11] Thus, it appears that it is this d-like component of the conduction-electron wave function which is strongly scattered by Fe impurities. Further, the region of strong scattering at [101] extends approximately 3 times as far toward [001] as toward [111] (Fig. 2), in good agreement with the general shape of the concave part of the Fermi surface. It is interesting that Dugdale and Bailyn have suggested[14] that the large negative phonon drag thermopowers which are observed when transition-metal impurities are added to gold might be explained if at low temperatures these impurities produce a large amount of scattering in the concave regions of the Fermi surface. Our results for Au:Fe provide rather direct experimental support for this suggestion, and in fact indicate that perhaps a similar argument will hold quite generally for noble-metal alloys having transition-metal solutes. Thus, we expect that de Haas–van Alphen maps of electronic lifetime anisotropy can be of direct use in understanding the effect of impurities, or of small amounts of any other lattice defects, on metallic transport coefficients.

It is emphasized that the maps in Figs. 1 and 2 are at present rather crude, based as they are on a set of five orbitally averaged electronic lifetimes for each type of scattering imperfection. They can readily be improved by extending the experiments to include a larger number of orbits in nonsymmetry directions, for each of which m^* in (5) may also be determined by the dHvA technique, and then to employ a more general fitting procedure such as that based on cubic harmonics as mentioned. Such work is currently in progress. These maps do however demonstrate convincingly the quite different electron scattering anisotropies in two cases where the scattering is dominated by a specified impurity. They also reveal that conclusions pertaining to scattering anisotropy based on orbital averages alone, for example, the ratio of neck to belly Dingle temperatures, can be misleading This is evidenced by reference to Fig. 2 from which it is seen that the electronic lifetime varies by ~5:1 around the ⟨111⟩ belly orbits.

---

*National Science Foundation Postdoctoral Fellow; present address: Department of Physics, University of Oregon, Eugene, Ore. 97403.

[1]M. R. Halse, Phil. Trans. Roy. Soc. London 265, 507 (1969).

[2]*Proceedings of an International Conference on Electron Mean Free Paths in Metals, Zurich, Switzerland, 1968* (Springer, Berlin, 1969); Phys. Kondens. Mater. 9, (1969).

[3]J. F. Koch and R. E. Doezema, Phys. Rev. Lett. 24, 507 (1970).

[4]T. G. Blaney and D. Parsons, J. Phys. C: Proc. Phys. Soc., London 3, 126 (1970).
[5]A. D. Brailsford, Phys. Rev. 149, 456 (1966).
[6]A. V. Gold, in *Electrons in Metals, Simon Fraser University Lectures, Solid State Physics, 1965,* edited by J. F. Cochran and R. R. Haering (Gordon and Breach, New York, 1968), Vol. I, p. 54.
[7]J. M. Ziman, Phys. Rev. 121, 1320 (1961).
[8]P. E. King-Smith, Phil. Mag. 12, 1123 (1965).
[9]P. T. Coleridge and I. M. Templeton, to be published.
[10]M. Springford, J. R. Stockton, and I. M. Templeton, Phys. Kondens. Mater. 9, 15 (1969).
[11]B. Segall, Phys. Rev. 125, 109 (1961).
[12]R. W. Morse, A. Myers, and C. T. Walker, J. Acoust. Soc. Amer. 33, 699 (1961).
[13]D. J. Roaf, Phil. Trans. Roy. Soc. London 255, 135 (1962).
[14]J. S. Dugdale and M. Bailyn, Phys. Rev. 157, 485 (1967).

EFFECTIVE ELECTRON AND HOLE INTERACTIONS IN A POLARIZABLE FIELD

S. D. Mahanti* and C. M. Varma
Bell Telephone Laboratories, Murray Hill, New Jersey 07974
(Received 10 August 1970)

The problem of exciton states is considered in the presence of the interactions of the electron and the hole with optical phonons. In the two limits exciton Bohr radius r_{ex} much smaller and much larger than the polaron radii $r_{e,h}$*, the problem can be solved exactly. An interpolation scheme for obtaining results for intermediate values of the parameter $r_{ex}/r_{e,h}$* is proposed. An effective nonlocal electron-hole potential is obtained which reduces to the physically expected results in various limits.

We consider the problem of an electron and a hole interacting with each other and with longitudinal optical phonons as a prototype of the problem of two particles interacting with a field. We are motivated by the availability of experimental results on electron-hole bound states—the excitons in ionic semiconductors. We confine our attention to the case that the exciton state has a binding energy E_B small compared with the insulating energy gap Δ (Wannier exciton limit). A number of experimental results[1] in this limit reveal the importance of optical phonons; for example the measured E_B for Wannier excitons in TlCl and TlBr are an order of magnitude different from that calculated by hydrogenic formula using either the static or optical (high frequency) dielectric constants. It is also equally away from the calculated value using the existing theoretical potential derived by Haken.[2]

Our method consists in examining the poles of the t matrix for electron-polaron (ep) and hole-polaron (hp) scattering due to Coulomb interactions and interactions mediated by phonons, since these poles occur at the bound states of the pair. The interaction between the electrons or holes and the phonons is represented by the Fröhlich Hamiltonian.[2] This many-body formalism has been outlined by Nozières[3] and has already been used by Sham and Rice[4] to derive the effective-mass equation for the Wannier excitons, considering only the Coulomb interactions between a bare electron and a hole.

The t matrix satisfies the Bethe-Salpeter (BS) equation whose homogeneous part may be written[3]

$$t(k,k';q)=\textstyle\sum_{k''} I(k,k'';q)G(k''-\frac{1}{2}q)G(k''+\frac{1}{2}q)t(k'',k';q). \tag{1}$$

In Eq. (1) $G(k)$ is the single-particle Green's function and $k\equiv(\vec{k},\zeta)$ is momentum-energy four-vector; $k=k_2-\frac{1}{2}q$, $k'=k_4-\frac{1}{2}q$, where k_2 and k_4 refer to the ingoing and outgoing electron and $q=(\vec{Q},\omega)$ is the total four-momentum carried by the electron-hole pair. Since k' and q are fixed parameters, we will use $t(k,k';q)\to T(k)$ for brevity. The single-particle Green's function G for ep and hp are given by the sum of the coherent and incoherent parts: $G=G_{\rm coh}+G_{\rm inc}$, where

$$G_{\rm coh}(\vec{k},\zeta)=\frac{Z_e(\vec{k})}{\zeta-E_e(\vec{k})+i\delta}+\frac{Z_h(\vec{k})}{\zeta-E_h(\vec{k})-i\delta}, \tag{2}$$

$$G_{\rm inc}(\vec{k},\zeta)=\int_{E_e(\vec{k})+\epsilon_e}^{\infty}\frac{\rho_e(\vec{k},E)}{\zeta-E}dE+\int_{E_h(\vec{k})-\epsilon_h}^{-\infty}\frac{\rho_h(\vec{k},E)}{\zeta-E}dE. \tag{3}$$

In (2),

$$E_e(\vec{k})=\Delta+k^2/2m_e+\Sigma_e(\vec{k},E_e(\vec{k})),\quad E_h(\vec{k})=-k^2/2m_h+\Sigma_h(\vec{k},E_h(\vec{k})), \tag{4}$$